


## Quantum charge pumping through Majorana bound states

Krashna Mohan Tripathi,<sup>1</sup> Sumathi Rao,<sup>1</sup> and Sourin Das<sup>2,3</sup>

<sup>1</sup>*Harish-Chandra Research Institute, HBNI, Chhatnag Road, Jhusi, Allahabad 211 019, India*

<sup>2</sup>*Department of Physical Sciences, Indian Institute of Science Education and Research, Kolkata, West Bengal, 741252, India*

<sup>3</sup>*Department of Physics and Astrophysics, University of Delhi, Delhi - 110 007, India*

 (Received 15 September 2018; revised manuscript received 26 January 2019; published 25 February 2019)

We study adiabatic charge pumping through a Majorana bound state tunnel coupled to multiple normal leads. We show that, for most of the parameters, such a pump does not lead to any net pumped charge between the various leads unless a multiply connected geometry is implemented. We introduce an Aharonov–Bohm ring geometry at the junction to implement such a multiply connected geometry. We further show that the Fourier transform of the pumped charge with respect to the flux inserted through the ring shows a clear distinction between the case of an Andreev bound state and the Majorana bound state. Hence such a Fourier analysis can serve as a diagnostic for the detection of Majorana bound states in the proposed geometry.

DOI: [10.1103/PhysRevB.99.085435](https://doi.org/10.1103/PhysRevB.99.085435)

### I. INTRODUCTION

One of the first steps that is required for the application of Majorana modes [1–3] in quantum computation is its unambiguous identification. This has proved difficult in experiments [4,5], since the usual diagnostic of Majorana bound states (MBSs), a zero-bias peak in the conductance, can have many other origins besides signaling the presence of a Majorana mode. This fact has led to considerable work [6] in recent years, encompassing the study of various toy models [7] and promising physical systems [8,9] and their electrical transport signatures [10].

However, there has been no definitive experimental confirmation so far which has proved the existence of Majorana modes in any system and hence it is still of interest to look for different ways to confirm the existence of Majorana modes. In this context, it is worth exploring the question of charge pumping through a Majorana mode and examining whether there are unique signals which can identify it and differentiate it from pumping through other resonant levels or Andreev bound states. Charge pumping or the phenomenon of obtaining current in the absence of bias by local variations of parameters of the quantum system has been studied in many contexts, beginning with Thouless [11] who considered the effect of a traveling periodic potential that could drag the electrons along. The analysis performed by Thouless was in the spirit of a closed quantum system.

Later the idea of pumping was extended to open quantum system in Refs. [12,13], where the pumping of charge is induced between different electron reservoirs by periodically varying the independent parameters of the scattering matrix that describes the scattering of electrons between the different electron reservoirs. When the variation of the parameters is much slower than the transport time, then the pumping is adiabatic and the Brouwer formula [13] can be applied. Adiabatic charge pumping has attracted a great deal of interest in the last several years, and different aspects of it have been studied in great detail [14–37]. There has also been some work

[38–49] on normal-metal–superconductor interfaces including Majorana [50–52] mediated charge pumps.

There has also been recent interest in cases when the pumped charge is quantized, and in particular for topological reasons [50], so that it is stable to disorder and could be used for metrological applications. As mentioned above, this was first studied by Thouless [11] who showed that the quantized adiabatic charge transport was related to the Chern number of the band, which also counts the number of monopoles or equivalently gapless points enclosed by the pumping contour. In recent work [50], it has been shown that the presence of a single transmitting channel at the interface between a normal wire and a superconductor enables quantization of the pumped charge by tuning the system through topological phase transitions so that isolated topologically trivial regions are surrounded by topological regions. Thus pumping paths can be chosen to make noncontractible loops in the parameter space which could lead to quantized charge pumping.

In an earlier paper [53], we studied the conductance through a Majorana bound state (MBS) embedded in an Aharonov–Bohm ring geometry and showed that the currents at the two leads tunnel coupled to the Aharonov–Bohm ring were anticorrelated and the degree of anticorrelation could be tuned by the Aharonov–Bohm ( $\mathcal{A}\mathcal{B}$ ) flux threading the ring. In this paper, we explore charge pumping through the MBS in the same geometry and study the role of the  $\mathcal{A}\mathcal{B}$  ring geometry, which exhibits nontrivial topology. Unlike Ref. [50], where the pumping of charge required going through topological phase transitions as one traverses along the pumping contour, here we show that it is possible to obtain quantized pumped charge even when the superconductor hosting the MBS does not undergo phase transitions.

The ring geometry plays a crucial role here since we will show that there is no pumped charge when the two leads are just connected to the MBS (normal-MBS-normal or simple two-lead geometry without the ring). This is unlike the earlier study of conductance [53] where the anticorrelation existed even in the two-lead geometry and the  $\mathcal{A}\mathcal{B}$  geometry

was required only to provide a tuning parameter for tuning the degree of anticorrelation. Here, on the contrary, the  $\mathcal{AB}$  geometry is crucial to get nonzero pumping. In this geometry, we study the pumped charge at each of the leads by using a scattering matrix approach, restricting ourselves to the adiabatic regime, and we compute the pumped charge by using the analog [39] of the Brouwer [13] formula for a normal-superconductor junction. Finally, we show that a Fourier analysis of the pumped charge as a function of the flux through the ring leads to a single frequency domination for the MBS, as opposed to many harmonics for an Andreev bound state (ABS); this can be thought of as a diagnostic for the MBS.

The paper is organized as follows: In Sec.(II), we study a two-normal-lead geometry, and show that, at zero energy, no charge is pumped through a MBS, but nonzero charge can be pumped through an ABS, both between the leads and from the leads to the superconductor. In Sec. III, we introduce the  $\mathcal{AB}$  geometry. We study pumping across a MBS and for contrast, a resonant level, and show that the symmetries of the derivatives of the  $S$  matrix with respect to the pumping parameters, determine whether charge can be pumped. In Sec. IV, we explicitly study the pumped charge for various representative contours and look for circumstances under which we can get quantized pumped charge. Finally, in Sec. V, we show that the Fourier transform of the pumped charge with respect to the flux inserted in the ring has a single periodicity for the MBS case, as opposed to the cases for the resonant level and for the ABS case. This can serve as a diagnostic for a MBS and unambiguously distinguish it from other accidental bound states. We end with a discussion and conclusions in Sec. VI.

## II. SIMPLE CONNECTED GEOMETRY WITH TWO LEADS

We start with a simplified minimal model to illustrate the physics. Here, this is given by the Hamiltonian for two normal leads which are tunnel coupled to a MBS situated at the end of a one-dimensional  $p$ -wave superconductor [54],

$$H = \sum_{\alpha} H_{\alpha} + H_T, \quad (1)$$

where the form of the lead Hamiltonian for the two ( $\alpha = 1, 2$ ) leads is given by  $H_{\alpha} = \int_{-\infty}^{\infty} dx \psi_{\alpha}^{\dagger}(x)(-iv_F \partial_x) \psi_{\alpha}(x)$  and the tunneling Hamiltonian is given by

$$H_T = i\gamma \sum_{\alpha} [u_{\alpha} \psi_{\alpha}(x=0) + u_{\alpha}^* \psi_{\alpha}^{\dagger}(x=0)]. \quad (2)$$

Here  $\gamma$  represents the Majorana fermion operator and  $u_{\alpha}$  represents the amplitude of the coupling between the lead  $\alpha$  and the MBS, which is a complex number in general. The scattering matrix describing the scattering of electrons and holes between the leads via the MBS corresponding to the situation described by the above tunnel Hamiltonian is found by applying the Weidenmuller formula [53] as

$$S(E) = \begin{pmatrix} S^{ee}(E) & S^{eh}(E) \\ S^{he}(E) & S^{hh}(E) \end{pmatrix}, \quad (3)$$

where

$$S^{ee}(E) = 1_2 - \frac{2i\pi v}{d(E)} \begin{pmatrix} |u_1|^2 & u_1^* u_2 \\ u_2^* u_1 & |u_2|^2 \end{pmatrix}, \\ S^{he}(E) = -\frac{2i\pi v}{d(E)} \begin{pmatrix} u_1^2 & u_1 u_2 \\ u_1 u_2 & u_2^2 \end{pmatrix}, \quad (4)$$

with  $d(E) = E + 2i\pi v(|u_1|^2 + |u_2|^2)$ . Here the scattering matrix is written in a basis where the first two rows and columns correspond to electrons from lead-1 and lead-2 respectively, and the next two rows and columns correspond to holes from lead-1 and lead-2 respectively, and  $v$  represents the density of states of the electrons which has been assumed to be the same in both leads for simplicity.

Using the extension of Brouwer's formula for the case of superconducting junction [39], the pumped charge at each lead is given by

$$Q_{\alpha} = -e \int_{\mathcal{A}} dX_1 dX_2 \text{Im}[C_{\alpha\alpha}] \quad (5)$$

where the matrix

$$C = \frac{1}{\pi} \left[ \frac{d}{dX_1} S^{ee} \frac{d}{dX_2} (S^{ee})^{\dagger} - \frac{d}{dX_1} S^{he} \frac{d}{dX_2} (S^{he})^{\dagger} \right]. \quad (6)$$

Here  $X_1$  and  $X_2$  represent the pumping parameters which are periodic functions of the time  $t$ . They trace out a closed loop in the  $X_1$ - $X_2$  plane over one time period such that the area enclosed by the loop is finite and is given by  $\mathcal{A}$ . Also note that the pumped charge in each lead can be decomposed into a particle-like process which depends on  $S^{ee}$  alone and a particle-hole conversion process which depends on  $S^{he}$  alone.

We can choose the  $u_{\alpha}$  to be the pumping parameters, i.e., we can choose  $X_1 = u_1$  and  $X_2 = u_2$ . In this case, we find that

$$\text{Im}[C_{11}] = 0 = \text{Im}[C_{22}], \quad (7)$$

i.e., the integrand itself vanishes and there is no pumped charge. Note that the  $u_{\alpha}$  can be taken to be real since their phase can be gauged away as long as it is not time dependent. Alternatively, if we intend to use the phase of the  $u_{\alpha}$  as a pumping parameter (i.e., make it time dependent), the implementation of such a pumping protocol requires the order parameter of the superconducting hosting the MBS to be varied in time, which in turn calls for a Josephson-junction-type setup, which is beyond the scope of the present work.

To contrast the case of MBS with a more regularly encountered bound state in the context of normal-superconducting hybrid structures, the Andreev bound state (ABS), we show now that the vanishing of the pumped charge is not true in general. When we couple an ABS to leads, we see that it leads to a finite pumped charge even when the ABS is tuned to zero energy. To evaluate the pumped charge via an ABS, we start by replacing the tunnel Hamiltonian in Eq. (2) by [53]

$$H_T = a^{\dagger} \sum_{\alpha,k} (t_{\alpha} c_{\alpha k} + v_{\alpha}^* c_{\alpha k}^{\dagger}) + \text{H.c.}, \quad (8)$$

where now  $a^{\dagger}$  denotes the creation operator for the ABS (which, unlike the MBS, does not have to be real) and the tunneling amplitudes to the electron and hole states on the leads are given by  $t_{\alpha}$  and  $v_{\alpha}^*$ , respectively. Considering  $t_1$  and

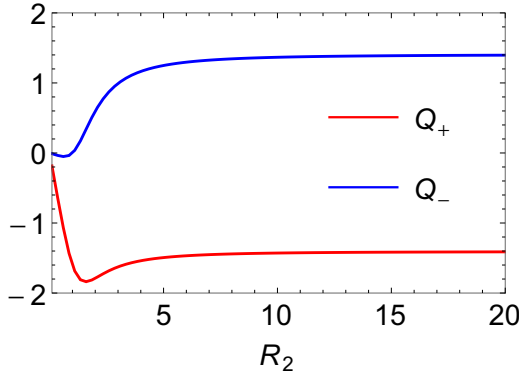


FIG. 1. The charge pumped to the superconductor, given by  $Q_+$ , is shown in blue while the charge pumped between the two normal leads through the ABS, given by  $Q_-$ , is shown in red (in the absence of the direct tunneling between the leads), in units of the electronic charge  $e$ . The pumping occurs in the  $t_1$ - $t_2$  plane and the pumped charge is shown as a function of a scale  $R_2$  which parametrizes the pumping contour as  $t_1^2 + t_2^2/R_2^2 = 1$ . The parameters  $v_1, v_2$  are chosen to be  $v_1 = 1, v_2 = i$ .

$t_2$  to be pumping parameters, and parametrizing the contour in terms of a scale  $R_2$  ( $t_1^2 + t_2^2/R_2^2 = 1$ ), we can obtain the pumped charge.

As the analytic expression for the pumped charge in this case gets cumbersome, we perform a numerical analysis for some representative values to obtain it by using Eqs. (5) and (6). This is presented in Fig. 1. Note that the total charge pumped from the normal metal leads into the superconductor is given by  $Q_+ = Q_1 + Q_2$  and the total charge pumped from lead-1 to lead-2 via the ABS is given by  $Q_- = Q_1 - Q_2$  over a single pumping cycle. We observe that both these quantities are finite for the chosen pumping contour and they asymptotically reach a steady value as the amplitude of pumping parameter  $R$  gets larger and larger. Hence, this fact itself presents a clear distinction between the ABS and MBS in this geometry.

### III. MULTIPLY CONNECTED GEOMETRY AND THE MAJORANA BOUND STATE

From the above analysis it is clear that a simple setup involving two leads tunnel coupled to a MBS does not lead to net charge being pumped either from one lead to another or from the leads to the superconductor over a pumping cycle. Next, we explore the possibility of pumping in a multiply connected geometry where the MBS is embedded in a ring.

*MBS embedded in an  $\mathcal{AB}$  geometry.* We now look for a multiply connected geometry and, once again, we make the simplest choice, which is to consider a ring geometry where a magnetic flux is piercing the ring. The ring geometry is realized by considering a MBS which is tunnel coupled to two leads that are also directly tunnel coupled to one another as shown in Fig. 2. The Hamiltonian for the system is the same as that given in Eq. (1) except that we now have an additional direct tunneling term given by

$$H_{\text{direct}} = \tau \psi_1^\dagger(x=0)\psi_2(x=0) + \text{H.c.} \quad (9)$$

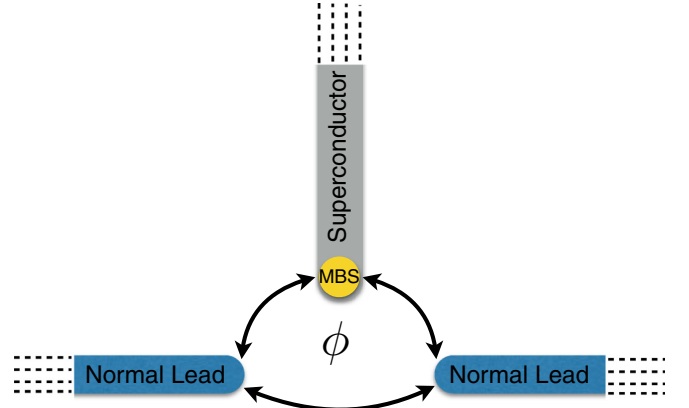


FIG. 2. Schematic illustration of the  $\mathcal{AB}$  setup with two normal leads, which are simultaneously tunnel coupled to the MBS and to each other. Here the tunnel coupling is represented as a double-headed arrow and the flux through the ring-type geometry is represented by  $\phi$ .

Here  $\tau$  denotes the amplitude for the direct tunnel coupling of the two leads to each other. The scattering matrix now involves the direct coupling term as well and is given by

$$S^{ee}(E) = \frac{1}{1 + \pi^2 v^2 |\tau|^2} \begin{pmatrix} 1 - \pi^2 v^2 |\tau|^2 & -2i\pi v \tau \\ -2i\pi v \tau^* & 1 - \pi^2 v^2 |\tau|^2 \end{pmatrix} - \frac{2i\pi v}{(1 + \pi^2 v^2 |\tau|^2)^2 D(E)} \begin{pmatrix} u_{1+}^* u_{1-} & u_{1+}^* u_{2-} \\ u_{2+}^* u_{1-} & u_{2+}^* u_{2-} \end{pmatrix}, \quad (10)$$

and

$$S^{he}(E) = -\frac{2i\pi v}{(1 + \pi^2 v^2 |\tau|^2)^2 D(E)} \begin{pmatrix} u_{1+} u_{1-} & u_{1+} u_{2-} \\ u_{2+} u_{1-} & u_{2+} u_{2-} \end{pmatrix}, \quad (11)$$

with  $D(E) = E + \frac{2i\pi v}{(1 + \pi^2 v^2 |\tau|^2)} (|u_1|^2 + |u_2|^2)$ ,  $u_{1s} = u_1 + si\pi v \tau^* u_2$ ,  $u_{2s} = u_2 + si\pi v \tau u_1$ , and  $s = +, -$ . Once again, the pumped charge for the pumping parameter being  $u_1, u_2$  can be computed by using the analog of Brouwer's formula. Here, we find that the integrand is given by

$$\text{Im}[C_{11}] = \frac{16\pi^2 v^3 \tau_0 (1 + \pi^2 v^2 \tau_0^2) \cos(\phi) E^2 (u_1^2 + u_2^2)}{[E^2 (1 + \pi^2 v^2 \tau_0^2)^2 + 4\pi^2 v^2 (u_1^2 + u_2^2)]^2} = -\text{Im}[C_{22}]. \quad (12)$$

As before, the  $u_\alpha$ s are taken to be real, and the direct tunneling term is taken to be  $\tau = \tau_0 e^{i\phi}$  where  $\phi$  plays the role of the  $\mathcal{AB}$  flux.

Clearly, this expression is zero when the direct tunneling amplitude is zero and it agrees with the earlier result. Using this in Eq. (5), we see that the integrand and, consequently, the pumped charge through each lead is zero even in the presence of a direct tunneling term, at  $E = 0$ .

So, although we have allowed for a finite direct tunneling amplitude  $\tau_0$  for the electrons, leading to a multiply connected geometry, we are still unable to obtain pumped charge at  $E = 0$ . The MBS in many aspects is very similar to a resonant level (RL). The MBS allows for resonant injection of a pair of electrons into a superconductor via a resonant Andreev

process and the RL allows for a single electron to resonantly transmit across it. Thus, to gain insight into the MBS pumping analysis, our next analysis is to consider pumping of charge across a RL embedded into an  $\mathcal{AB}$  geometry.

*AB geometry and the resonant level.* We can now contrast the above observed behavior of the MBS to the case where the MBS is replaced by a RL. The only change in the above model is that the first line of the tunneling term in Eq. (2) that represents tunneling through the MBS is now replaced by

$$H_T = \left( d^\dagger \sum_{\alpha} u_{\alpha} \psi_{\alpha}(x=0) + \text{H.c.} \right), \quad (13)$$

where  $d^\dagger$  represents the creation operator of the electron on the resonant level. The direct coupling term between the leads remains the same. The scattering matrix in this case is given by

$$\begin{aligned} S(E) &= \begin{pmatrix} S_{11}(E) & S_{12}(E) \\ S_{21}(E) & S_{22}(E) \end{pmatrix}, \\ S_{ij;i=j}(E) &= -1 + \frac{2(E + i\pi v u_{ij})}{\tilde{d}(E)}, \\ S_{ij;i \neq j}(E) &= -\frac{2i\pi v(E\tau_0 e^{i\phi_{ij}} + u_1 u_2)}{\tilde{d}(E)}, \\ \tilde{d}(E) &= E(1 + \pi^2 v^2 \tau_0^2) + 2\pi^2 v^2 \tau_0 \cos(\phi) u_1 u_2 \\ &\quad + i\pi v(u_1^2 + u_2^2), \end{aligned} \quad (14)$$

where  $u_{11} = u_2^2$ ,  $u_{22} = u_1^2$  and  $\phi_{12} = \phi$ ,  $\phi_{21} = -\phi$ . Now the pumped charge can be evaluated from the expressions for  $\text{Im}[C_{11}]$  and  $\text{Im}[C_{22}]$  as given below,

$$\begin{aligned} \text{Im}[C_{11}] &= \frac{8\pi^2 v^3}{|d(E)|^4} (u_1^2 + u_2^2) (E^2 \tau_0 \cos(\phi) (1 + \pi^2 v^2 \tau_0^2) \\ &\quad + E \{ u_1 u_2 [1 + \pi^2 v^2 \tau_0^2 \cos(2\phi)] \\ &\quad - \pi v \tau_0 \sin(\phi) (u_1^2 - u_2^2) \}) \\ &= -\text{Im}[C_{22}]. \end{aligned} \quad (15)$$

Note that, unlike the MBS case, where the integrand vanishes without direct tunneling between the leads, here the integrand is nonzero even for  $\tau_0 = 0$ . This clearly indicates that, although the direct tunneling term or the ring geometry was absolutely necessary to even get a nonzero integrand for the MBS case, that is not the case for the RL case. However, the pumped charge through each lead continues to be identically zero in both cases at  $E = 0$  [37].

*AB geometry and the role of pumping parameters.* We note above that, for both the MBS and the RL, the pumped charge is zero at  $E = 0$ , while it is finite in general for ABS. Thus it is natural to ask whether the choice of pumping parameters can change this fact. For the case of the MBS embedded in a ring we replace the pumping parameter  $u_2$ , which is one of the hopping amplitudes to the MBS, by  $\bar{\tau}_0 = \pi v \tau_0$  which is the amplitude for direct tunneling between the leads. Note that this explicitly breaks the symmetry between the two leads as far as the pumping contour is concerned. In this case, we find that even at  $E = 0$  the integrand is finite and is

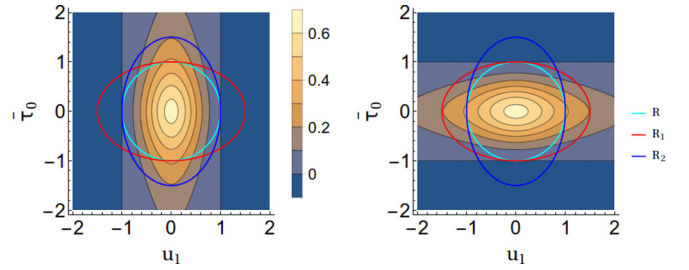


FIG. 3. The integrands  $\text{Im}(C_{11} + C_{22})$  and  $\text{Im}(C_{22} - C_{11})$  plotted as a function of the pumping parameters  $u_1$  and  $\bar{\tau}_0$ . Here, we have taken  $u_2 = 1$  and the phase of the direct hopping  $\phi = 0$ . The three contours  $a$ ,  $b$ , and  $c$  (explained in the text) for which we have computed the pumped charges  $Q_+$  and  $Q_-$  in Fig. (4) are shown in cyan, blue, and red, respectively.

given by

$$\begin{aligned} \text{Im}[C_{11}] &= \frac{2 \cos(\phi) u_2 [u_1^2 - \bar{\tau}_0^2 u_2^2]}{\pi (u_1^2 + u_2^2)^2 (1 + \bar{\tau}_0^2)^2}, \\ \text{Im}[C_{22}] &= -\frac{2 \cos(\phi) u_2 [u_2^2 - \bar{\tau}_0^2 u_1^2]}{\pi (u_1^2 + u_2^2)^2 (1 + \bar{\tau}_0^2)^2}. \end{aligned} \quad (16)$$

In Fig. 3, we show a plot of the integrands  $\text{Im}(C_{11} + C_{22})$  and  $\text{Im}(C_{22} - C_{11})$  as a function of the two pumping parameters. The pumped charge at the two leads can now be computed by choosing various contours. We show below the pumped charge for a few representative contours and note how asymptotically, (almost) quantized charge is pumped either to the superconductor or between the two leads.

*Symmetry arguments in the AB geometry.* Note that the particle-hole symmetry of the Bogoliubov–de Gennes Hamiltonian implies that the spectrum is symmetric around  $E = 0$ . The scattering matrix respects this symmetry, i.e.,  $S^{hh}(E) = [S^{ee}(-E)]^*$ ,  $S^{eh}(E) = [S^{he}(-E)]^*$ , for both the MBS as well as the ABS for all cases. However, as explained in detail in Ref. [53], the  $E = 0$  ABS is not self-conjugate and leads to differences between the MBS and ABS, even at the conductance level in an  $\mathcal{AB}$  geometry. But for charge pumping, it is not merely the symmetries of the scattering matrix which are important. Instead, the pumping depends on the convolution of the symmetries of the  $S$  matrix and its derivatives; hence the choice of pumping parameters are crucial in determining whether charge can be pumped. Without a ring geometry, when we try to pump charge via a Majorana bound state, the probability of pumping an electron through the Majorana is almost always equal to the probability of pumping a hole through the Majorana, thus resulting in zero net pumped charge. But a ring geometry allows for interference effects between transport across the MBS and the additional direct transport between the two leads and the total pumped charge from one lead to the other is clearly equal to the sum of contributions due to tunneling through the Majorana, tunneling through the direct path and their interference. The presence of this interference term is actually what is responsible for the finite pumped charge. The interference term essentially ensures that  $\text{Im}[C_{11}]$ ,  $\text{Im}[C_{22}]$  (directly proportional to the pumped charge) remain finite. However, just the presence of



the interference term is not enough to ensure that the pumped charge across the ring will be finite at zero energy. To ensure that the pumped charge is finite at  $E = 0$  we have to obtain a finite contribution to  $\text{Im}[C_{11}]$ ,  $\text{Im}[C_{22}]$  which is nonvanishing at  $E = 0$ . The choice of the  $u_1$ ,  $u_2$  pumping parameters results in a finite  $\text{Im}[C_{11}]$ ,  $\text{Im}[C_{22}]$  for  $E \neq 0$  but it vanishes for  $E = 0$  due to the symmetry of the derivatives of the  $S$  matrix under  $u_1 \leftrightarrow u_2$ . This symmetry is broken by choosing  $\tau$  as one of the pumping parameters, while  $u_{1/2}$  is chosen as the other pumping parameter.

#### IV. PUMPED CHARGE FOR VARIOUS PUMPING CONTOURS

In this section, we study pumped charge for different representative pumping contours and see when we get maximum pumped charge. As the physically relevant quantities are  $Q_+$  and  $Q_-$ , we first plot the integrands  $\text{Im}(C_{11} + C_{22})$  and  $\text{Im}(C_{22} - C_{11})$  as a function of the pumping parameters  $u_1$  and  $\bar{\tau}_0$  as shown in Fig. 3. Note that the maximum value for  $Q_+$  and  $-Q_-$  are concentrated about the  $u_1 = 0$  and  $\bar{\tau}_0 = 0$  axes, respectively. Also, note that the sign of  $\text{Im}(C_{11} + C_{22})$  and  $\text{Im}(C_{22} - C_{11})$  remains the same as we move along the axis about which the maxima of these functions are mostly distributed. On the other hand  $\text{Im}(C_{11} + C_{22})$  and  $\text{Im}(C_{22} - C_{11})$  do change sign along the axis perpendicular to the axis of the distribution of the maxima. This fact will strongly influence the asymptotic values of the pumped charge as we go to larger and larger contour sizes. For obtaining large values of pumped charge we need to analyze the symmetries of the distribution of values of  $\text{Im}(C_{11} + C_{22})$  and  $\text{Im}(C_{22} - C_{11})$  and design pumping contours which will efficiently enclose a large fraction of the maxima of these functions in the parameter space. In principle, appropriately chosen contours can lead to asymptotically quantized value for pumped charge [17,29,31,36,47]. Keeping this fact in mind we consider elliptical shapes of the contours in the plane of the pumping parameters ( $u_1, \bar{\tau}_0$ ) given by  $u_1^2/R_1^2 + \bar{\tau}_0^2/R_2^2 = 1$ .

We have produced plots for three different kinds of contours which are given by (a)  $R_1 = R_2 = R$  where the asymptotic pumped charge is obtained for  $R \rightarrow \infty$  limit, (b)  $R_2/R_1 > 1$  where the asymptotic pumped charge is obtained for the  $R_2 \rightarrow \infty$  limit, and (c)  $R_1/R_2 > 1$  where the asymptotic pumped charge is obtained for the  $R_1 \rightarrow \infty$  limit. In Fig. 3 we have shown representative contours for the cases (a), (b), and (c) discussed above in cyan, blue, and red respectively. The corresponding asymptotic pumped charge is given in Fig. 4 where the color code of corresponding cases are kept the same.

Let us first discuss the results corresponding to the (b)-type contour which is depicted in blue in Figs. 3 and 4. We note that  $Q_+ \rightarrow 2$ , i.e., gets asymptotically quantized while  $Q_- \rightarrow 0$  as  $R_2 \rightarrow \infty$ . This fact is consistent with our observation that the maximum of  $\text{Im}(C_{11} + C_{22})$  is distributed around the  $u_1 = 0$  axis and the (b)-type contour maximally encloses the area around this axis, hence leading to quantization of  $Q_+$ . On the other hand,  $\text{Im}(C_{22} - C_{11})$  changes sign as we move along the  $u_1 = 0$  axis and hence  $Q_-$  shows a nonmonotonic behavior and finally goes to zero as  $R_2 \rightarrow \infty$ .

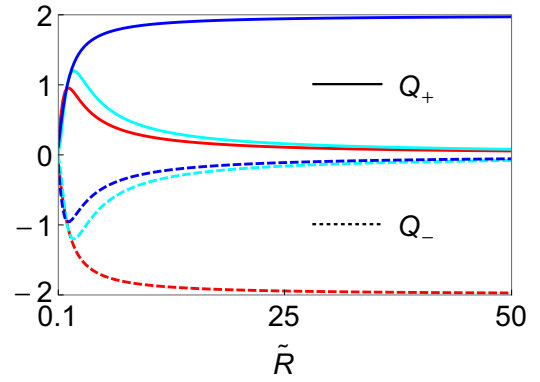


FIG. 4. Pumped charges to the superconductor ( $Q_+$ ) and between the leads ( $Q_-$ ) for the MBS in the presence of direct tunneling in units of electronic charge  $e$  for pumping in  $u_1$ - $\bar{\tau}_0$  plane as a function of the scale of the relative pumping strengths (the elliptic contours) and the radius for equal pumping strengths (circular contour). More explicitly, the variable  $\tilde{R}$  which labels the  $x$  axis denotes  $R$ ,  $R_1$ , and  $R_2$  respectively for the contours (a), (b), and (c), respectively. The parameter  $u_2$  is chosen to be  $u_2 = 1$ .

The same logic can be used to understand the fact that the (a)-type contour always shows a nonmonotonic behavior for the pumped charge which always goes to zero in the asymptotic limit. This is so because the (a)-type contour always engulfs areas where  $\text{Im}(C_{11} + C_{22})$  and  $\text{Im}(C_{22} - C_{11})$  both undergo sign changes, hence canceling to zero in the asymptotic limit. Finally it is clear from the above arguments that the (c)-type contour will show a behavior which is exactly complementary to the (b)-type contour since the maximum values of  $\text{Im}(C_{11} + C_{22})$  and  $\text{Im}(C_{22} - C_{11})$  are distributed around complementary axis (i.e., the  $u_1 = 0$  and  $\bar{\tau}_0 = 0$  axes, respectively). Hence we have shown that, by choosing appropriate contours, we are in a position to selectively pump charge from the leads to the superconductor ( $Q_+ \neq 0$ ) while keeping the relative transfer of charge between the leads to be zero ( $Q_- = 0$ ) or pump charge between the leads ( $Q_- \neq 0$ ) while keeping the superconductor decoupled [i.e., keeping ( $Q_+ = 0$ )].

#### V. FOURIER ANALYSIS OF PUMPED CHARGE

Finally, in this section, we would like to point out a crucial difference in the scattering matrix for the MBS in the multiply connected geometry and the scattering matrix for other forms of bound states like the ABS or the RL in the same geometry. The other forms of bound states, in general, lead to a  $\phi$ -dependent denominator which appears due to the Fabry-Pérot-type interference due to the circulating paths of electrons or holes around the multiply connected geometry. But due to the fine-tuned symmetry between an electron and a hole for the MBS, all such phases cancel out to provide a  $\phi$ -independent denominator. This can be seen clearly by comparing the expression for  $D(E)$  in Eq. (11) with  $\tilde{d}(E)$  in Eq. (14). Also note that the  $\phi$  dependence for the MBS appears only in the numerator of the scattering matrix as a pure cosine. The same difference in dependence on  $\phi$  also persists in the expression for the integrand of the

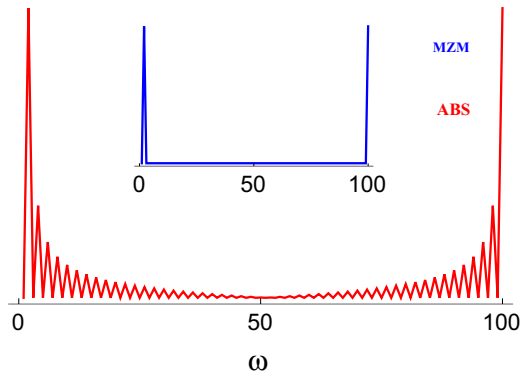


FIG. 5. Plot of discrete Fourier transform of  $Q_+$ ,  $|A(\omega)|^2 = |\frac{1}{N} \sum_{\phi} Q[\phi] e^{i2\pi * \omega \phi / N}|^2$  as a function of the frequency  $\omega$  for pumping in  $u_1 - \bar{v}_0$  plane for ABS in red and MBS in blue. The contour is chosen to be circular with  $R = 25$ . The number of points  $N$  is chosen to be 100 and the other parameters are given by  $u_2 = 1$ ,  $v_1 = 3$ ,  $v_2 = 2$ .

pumped charge, as can be seen from Eqs. (15) and (16). This essentially means that the pumped charge for the MBS has a single periodicity in  $\phi$ . In other words, the interference in the case of the MBS can be interpreted as Mach-Zehnder-like interference while in the other case, the interference is more akin to a Fabry-Pérot interferometer.

This difference can serve as a diagnostic for the MBS. This fact can be seen very clearly from the Fourier analysis for the pumped charge shown in Fig. 5. As expected, the MBS case show a clear  $\delta$ -function-like peak which is independent of the parameters chosen for the analysis due to the fact that only the first of the harmonics contributes to this case, whereas for the ABS, there are multiple frequencies signifying the presence of higher harmonics which can be traced back to the  $\phi$ -dependent expression for  $\tilde{d}(E)$ .

## VI. DISCUSSIONS AND CONCLUSION

We end with some suggestions of possible directions in which this research could be extended and possible experimental realizations of a charge pump. One direction would be to study the full low-energy Hamiltonian including the Majorana mode at the other end of the topological superconductor and take the finite size of the topological superconductor into account. One could then check whether charge pumping could be used as a measure of the splitting of the zero mode. Other possibilities would be to study heat pumping in this geometry. There has been recent work on heat pumping [55] in the usual two-lead geometry, where charge cannot be pumped; however,

here it may be interesting to see it in a situation where charge is also pumped.

We also note that, in this geometry, the possibility of distinguishing pumping from rectification effects using the suggestion in Ref. [56] is not feasible. There, it was suggested that an out-of-plane magnetic field could distinguish between the two, since rectification is symmetric under the change in sign of this magnetic field, whereas pumping is not. But in our geometry, the magnetic-flux dependence of the pumped charge through the MBS is also symmetric under reversal of sign of the applied magnetic field (or the magnetic flux), just like the rectification current. Hence, this symmetry does not provide a possible way to distinguish between the two. But we also predict a very specific dependence of the Fourier transform of the pumped charge with respect to the magnetic flux and this should be sufficient to distinguish between rectification effects and quantum charge-pumping effects.

However, regarding experimental verification, the crucial point here is the possibility of implementing an  $\mathcal{AB}$  ring geometry with wires that host Majorana modes. We note that, besides possible implementation of such a ring geometry using semiconductor or carbon nanotube quantum wires, following recent work on two-dimensional (2D) topological charge pumps in ultracold bosonic systems [57], it may even be possible to implement ring geometries in cold atom systems. However, more realistic feasibility studies are beyond the scope of this work.

In conclusion, in this paper, we have discussed the importance of a ring geometry to get nonzero pumped charge through the MBS. We note that, asymptotically, two units of charge can either be pumped between the leads or from the leads to the superconductor. We do not get quantized single-unit charge pumping within our setup, because our pumping protocol only involves the Majorana bound state at one end of the topological superconductor. Hence, the fermion parity is fixed. We then show that the Fourier analysis of the pumped charge through an  $\mathcal{AB}$  ring can be used as a diagnostic to distinguish between MBS from other spurious zero-energy states. In particular, the charge pumped through the MBS is different from the charge pumped through either the resonant level or the ABS in that it has no higher harmonics. This is true independent of choice of the contour and is consequently a strong diagnostic.

## ACKNOWLEDGMENT

The research of K.M.T. was supported in part by the INFOSYS scholarship for senior students.

- [1] J. Alicea, *Rep. Prog. Phys.* **75**, 076501 (2012).
- [2] C. W. J. Beenakker, *Annu. Rev. Condens. Matter Phys.* **4**, 113 (2013).
- [3] R. Aguado, *Riv. Nuovo Cimento* **40**, 523 (2017).
- [4] V. Mourik, K. Zuo, S. M. Frolov, S. R. Plissard, E. P. A. M. Bakkers, and L. P. Kouwenhoven, *Science* **336**, 1003 (2012).
- [5] M. T. Deng *et al.*, *Nano Lett.* **12**, 6414 (2012); A. Das *et al.*, *Nat. Phys.* **8**, 887 (2012); L. P. Rokhinson, X. Liu, and J. K. Furdyna,

- ibid.* **8**, 795 (2012); A. D. K. Finck, D. J. Van Harlingen, P. K. Mohseni, K. Jung, and X. Li, *Phys. Rev. Lett.* **110**, 126406 (2013); S. Nadj-Perge *et al.*, *Science* **346**, 602 (2014); R. Pawlak *et al.*, *npj Quantum Information* **2**, 16035 (2016); M. Ruby *et al.*, *Phys. Rev. Lett.* **115**, 197204 (2015).
- [6] D. Sen and S. Vishweshwara, *Europhys. Lett.* **91**, 66009 (2010); W. DeGottardi, D. Sen, and S. Vishweshwara, *New J. Phys.* **13**, 065028 (2011); P. W. Brouwer, M. Duckheim, A. Romito,

- and F. von Oppen, *Phys. Rev. Lett.* **107**, 196804 (2011); *Phys. Rev. B* **84**, 144526 (2011); S. Gangadharaiah, B. Braunecker, P. Simon, and D. Loss, *Phys. Rev. Lett.* **107**, 036801 (2011); B. H. Wu and J. C. Cao, *Phys. Rev. B* **85**, 085415 (2012); M. Leijnse and K. Flensberg, *Semicond. Sci. Technol.* **27**, 124003 (2012); H. F. Lu, H. Z. Lu, and S. Q. Shen, *Phys. Rev. B* **86**, 075318 (2012); B. Zocher and B. Rosenow, *Phys. Rev. Lett.* **111**, 036802 (2013).
- [7] Y. Oreg, G. Refael, and F. von Oppen, *Phys. Rev. Lett.* **105**, 177002 (2010); I. C. Fulga, F. Hassler, A. R. Akhmerov, and C. W. J. Beenakker, *Phys. Rev. B* **83**, 155429 (2011); A. R. Akhmerov, J. P. Dahlhaus, F. Hassler, M. Wimmer, and C. W. J. Beenakker, *Phys. Rev. Lett.* **106**, 057001 (2011); P. Wang, Y. Cao, M. Gong, G. Xiong, and X. Q. Li, *Europhys. Lett.* **103**, 57016 (2013).
- [8] L. Fu and C. L. Kane, *Phys. Rev. Lett.* **100**, 096407 (2008).
- [9] J. D. Sau, R. M. Lutchyn, S. Tewari, and S. Das Sarma, *Phys. Rev. Lett.* **104**, 040502 (2010); T. Stanescu and S. Tewari, *J. Phys.: Condens. Matter* **25**, 233201 (2013).
- [10] E. Wiesenmayer, H. Luetkens, G. Pascua, R. Khasanov, A. Amato, H. Potts, B. Bannusch, H.-H. Klauss, and D. Johrendt, *Phys. Rev. Lett.* **107**, 237001 (2011); A. Golub and B. Horowitz, *Phys. Rev. B* **83**, 153415 (2011); A. Haim, E. Berg, F. von Oppen, and Y. Oreg, *Phys. Rev. Lett.* **114**, 166406 (2015); *Phys. Rev. B* **92**, 245112 (2015).
- [11] D. J. Thouless, *Phys. Rev. B* **27**, 6083 (1983).
- [12] M. Buttiker, H. Thomas, and A. Pretre, *Z. Phys. B: Condens. Matter* **94**, 133 (1994).
- [13] P. W. Brouwer, *Phys. Rev. B* **58**, R10135(R) (1998).
- [14] I. L. Aleiner and A. V. Andreev, *Phys. Rev. Lett.* **81**, 1286 (1998).
- [15] F. Zhou, B. Spivak, and B. Altshuler, *Phys. Rev. Lett.* **82**, 608 (1999).
- [16] Y. Wei, J. Wang, and H. Guo, *Phys. Rev. B* **62**, 9947 (2000).
- [17] Y. Levinson, O. Entin-Wohlman, and P. Wolfle, *Phys. A (Amsterdam, Neth.)* **302**, 335 (2001).
- [18] F. Renzoni and T. Brandes, *Phys. Rev. B* **64**, 245301 (2001).
- [19] M. Blaauboer and E. J. Heller, *Phys. Rev. B* **64**, 241301(R) (2001).
- [20] M. L. Polianski and P. W. Brouwer, *Phys. Rev. B* **64**, 075304 (2001).
- [21] J. E. Avron, A. Elgart, G. M. Graf, and L. Sadun, *Phys. Rev. Lett.* **87**, 236601 (2001).
- [22] O. Entin-Wohlman, A. Aharony, and Y. Levinson, *Phys. Rev. B* **65**, 195411 (2002).
- [23] A. Aharony and O. Entin-Wohlman, *Phys. Rev. B* **65**, 241401(R) (2002).
- [24] J. N. H. J. Cremers and P. W. Brouwer, *Phys. Rev. B* **65**, 115333 (2002).
- [25] M. L. Polianski, M. G. Vavilov, and P. W. Brouwer, *Phys. Rev. B* **65**, 245314 (2002).
- [26] M. Moskalets and M. Buttiker, *Phys. Rev. B* **66**, 205320 (2002).
- [27] P. Sharma and C. Chamon, *Phys. Rev. B* **68**, 035321 (2003).
- [28] R. Citro, N. Andrei, and Q. Niu, *Phys. Rev. B* **68**, 165312 (2003).
- [29] A. Banerjee, S. Das, and S. Rao, [arXiv:cond-mat/0307324](https://arxiv.org/abs/cond-mat/0307324).
- [30] M. Moskalets and M. Buttiker, *Phys. Rev. B* **69**, 205316 (2004).
- [31] S. Das and S. Rao, *Phys. Rev. B* **70**, 155420 (2004).
- [32] E. Sela and Y. Oreg, *Phys. Rev. B* **71**, 075322 (2005).
- [33] J. Splettstoesser, M. Governale, J. König, and R. Fazio, *Phys. Rev. Lett.* **95**, 246803 (2005).
- [34] S. Banerjee, A. Mukherjee, S. Rao, and A. Saha, *Phys. Rev. B* **75**, 153407 (2007).
- [35] A. Agarwal and D. Sen, *Phys. Rev. B* **76**, 035308 (2007).
- [36] S. Das and V. Shpitalnik, *Europhys. Lett.* **83**, 17004 (2008).
- [37] H. K. Yadalam and U. Harbola, *Phys. Rev. B* **93**, 035312 (2016).
- [38] J. Wang, Y. Wei, B. Wang, and H. Guo, *Appl. Phys. Lett.* **79**, 3977 (2001).
- [39] M. Blaauboer, *Phys. Rev. B* **65**, 235318 (2002).
- [40] J. Wang and B. Wang, *Phys. Rev. B* **65**, 153311 (2002).
- [41] B. Wang and J. Wang, *Phys. Rev. B* **66**, 201305 (2002).
- [42] F. Taddei, M. Governale, and R. Fazio, *Phys. Rev. B* **70**, 052510 (2004).
- [43] M. Governale, F. Taddei, R. Fazio, and F. W. J. Hekking, *Phys. Rev. Lett.* **95**, 256801 (2005).
- [44] N. B. Kopnin, A. S. Melnikov, and V. M. Vinokur, *Phys. Rev. Lett.* **96**, 146802 (2006).
- [45] J. Splettstoesser, M. Governale, J. König, F. Taddei, and R. Fazio, *Phys. Rev. B* **75**, 235302 (2007).
- [46] S. Russo, J. Tobiska, T. M. Klapwijk, and A. F. Morpurgo, *Phys. Rev. Lett.* **99**, 086601 (2007).
- [47] A. Saha and S. Das, *Phys. Rev. B* **78**, 075412 (2008).
- [48] Ganesh C. Paul and Arijit Saha, *Phys. Rev. B* **95**, 045420 (2017).
- [49] F. W. J. Hekking and Y. V. Nazarov, *Phys. Rev. Lett.* **71**, 1625 (1993).
- [50] M. Gibertini, R. Fazio, M. Polini, and F. Taddei, *Phys. Rev. B* **88**, 140508(R) (2013).
- [51] M. Alos-Palop, R. P. Tiwari, and M. Blaauboer, *Phys. Rev. B* **89**, 045307 (2014).
- [52] Y. Herasymenko, K. Snizhko, and Y. Gefen, *Phys. Rev. Lett.* **120**, 226802 (2018).
- [53] K. M. Tripathi, S. Das, and S. Rao, *Phys. Rev. Lett.* **116**, 166401 (2016).
- [54] A. Kitaev, *Phys.-Usp.* **44** 131 (2001).
- [55] D. Meidan, T. Gur, and A. Romito, [arXiv:1807.06856](https://arxiv.org/abs/1807.06856).
- [56] P. W. Brouwer, *Phys. Rev. B* **63**, 121303 (2001).
- [57] M. Lohse, C. Schweizer, H. M. Price, O. Zilberberg, and I. Bloch, *Nature (London)* **553**, 55 (2018).